

Wnt10b Increases Postnatal Bone Formation by Enhancing Osteoblast Differentiation

Christina N Bennett,^{1,2} Hongjiao Ouyang,^{2,3} Yanfei L Ma,⁴ Qingqiang Zeng,⁴ Isabelle Gerin,¹ Kyle M Sousa,¹ Timothy F Lane,⁵ Venkatesh Krishnan,⁴ Kurt D Hankenson,⁶ and Ormond A MacDougald¹

ABSTRACT: Overexpression of Wnt10b from the osteocalcin promoter in transgenic mice increases postnatal bone mass. Increases in osteoblast perimeter, mineralizing surface, and bone formation rate without detectable changes in pre-osteoblast proliferation, osteoblast apoptosis, or osteoclast number and activity suggest that, in this animal model, Wnt10b primarily increases bone mass by stimulating osteoblastogenesis.

Introduction: Wnt signaling regulates many aspects of development including postnatal accrual of bone. Potential mechanisms for how Wnt signaling increases bone mass include regulation of osteoblast and/or osteoclast number and activity. To help differentiate between these possibilities, we studied mice in which Wnt10b is expressed specifically in osteoblast lineage cells or in mice devoid of Wnt10b.

Materials and Methods: Transgenic mice, in which mouse Wnt10b is expressed from the human osteocalcin promoter (Oc-Wnt10b), were generated in C57BL/6 mice. Transgene expression was evaluated by RNase protection assay. Quantitative assessment of bone variables was done by radiography, μ CT, and static and dynamic histomorphometry. Mechanisms of bone homeostasis were evaluated with assays for BrdU, TUNEL, and TRACP5b activity, as well as serum levels of C-terminal telopeptide of type I collagen (CTX). The endogenous role of Wnt10b in bone was assessed by dynamic histomorphometry in Wnt10b^{-/-} mice.

Results: Oc-Wnt10b mice have increased mandibular bone and impaired eruption of incisors during postnatal development. Analyses of femoral distal metaphyses show significantly higher BMD, bone volume fraction, and trabecular number. Increased bone formation is caused by increases in number of osteoblasts per bone surface, rate of mineral apposition, and percent mineralizing surface. Although number of osteoclasts per bone surface is not altered, Oc-Wnt10b mice have increased total osteoclast activity because of higher bone mass. In Wnt10b^{-/-} mice, changes in mineralizing variables and osteoblast perimeter in femoral distal metaphyses were not observed; however, bone formation rate is reduced because of decreased total bone volume and trabecular number.

Conclusions: High bone mass in Oc-Wnt10b mice is primarily caused by increased osteoblastogenesis, with a minor contribution from elevated mineralizing activity of osteoblasts.

J Bone Miner Res 2007;22:1924–1932. Published online on August 20, 2007; doi: 10.1359/JBMR.070810

Key words: osteocalcin, stromal cells, Wnt, mesenchymal, mandible

INTRODUCTION

OSTEOPOROSIS IS A disease characterized by pathologically low bone mass and elevated risk of fracture. Although development of osteoporosis is commonly associated with aging and menopause, genetic mutations have been identified that cause osteoporosis and/or contribute to its severity.^(1,2) For instance, development of osteoporosis pseudoglioma⁽³⁾ and juvenile osteoporosis⁽⁴⁾ is caused by inactivating mutations in low-density lipoprotein receptor-

related protein 5 (LRP5), a co-receptor for the Wnt signaling pathway.⁽⁵⁾ Furthermore, genetic analyses of kindred populations with high or low bone mass have identified activating⁽⁶⁾ and missense^(7,8) mutations in Lrp5, respectively. Thus, understanding mechanisms by which Wnt signaling regulates bone remodeling may help identify suitable targets for drug therapy of bone diseases.

The canonical Wnt signaling pathway is initiated when Wnts, a family of 19 secreted glycoproteins, bind to frizzled receptors⁽⁹⁾ and LRP co-receptors at the cell membrane.^(10–12) Transmission of the intracellular Wnt signal is still under study but involves interactions of frizzled with

The authors state that they have no conflicts of interest.

¹Department of Molecular and Integrative Physiology, University of Michigan Medical School, Ann Arbor, Michigan, USA; ²These authors contributed equally to this manuscript; ³The Bone Center, Department of Medicine, School of Medicine and School of Dentistry, University of Pittsburgh, Pittsburgh, Pennsylvania, USA; ⁴Eli Lilly and Company, Indianapolis, Indiana, USA; ⁵UCLA's Jonsson Comprehensive Cancer Center, University of California, Los Angeles, California, USA; ⁶Department of Orthopedic Surgery, University of Michigan Medical School, Ann Arbor, Michigan, USA.

disheveled and LRP5/6 with axin,^(13,14) which promotes disassociation of a protein complex that, in the absence of Wnt signaling, phosphorylates β -catenin and targets it for ubiquitin-mediated degradation.^(15–17) With active Wnt signaling, β -catenin accumulates in the cytosol and translocates to the nucleus where it promotes Tcf/Lef mediated transcription.⁽¹⁸⁾ A number of proteins antagonize the Wnt signaling pathway including secreted frizzled-related proteins (sFRPs), Wnt inhibitory factor, dickkopf, sclerostin, and chibby.^(19–23) Therefore, effects of Wnt signaling in bone homeostasis are potentially influenced by expression of Wnts, Wnt receptors, Wnt inhibitors, and downstream signaling components.

Our previous work suggests that activation of Wnt signaling in mesenchymal precursors stimulates osteoblastogenesis and inhibits adipogenesis.⁽²⁴⁾ Temporal and genetic analyses suggest that Wnt signaling alters cell fate predominantly by suppressing expression of adipogenic transcription factors.⁽²⁵⁾ Moreover, we found that Wnt10b is an endogenous regulator of bone mass.⁽²⁴⁾ In Wnt10b^{-/-} mice, distal metaphyses of femurs have ~30% less bone volume fraction and mineral density than femurs in wildtype mice. Furthermore, transgenic mice that express Wnt10b in bone marrow and adipose tissues from the FABP4 promoter (FABP4-Wnt10b) have increased trabecular bone volume and are resistant to bone loss associated with estrogen depletion or aging. FABP4-Wnt10b mice are also genetically lean, with ~50% reduction in adipose tissue mass and serum leptin, and are resistant to diet-induced obesity.⁽²⁶⁾ Mechanistic analyses of how Wnt10b directly increases bone mass in FABP4-Wnt10b mice are complicated by reduced leptin, which indirectly regulates bone formation through a hypothalamic loop involving sympathetic activation to bone marrow.^(27,28) In addition, activation of Wnt signaling has been proposed to increase bone mass through a number of mechanisms involving both osteoblasts and osteoclasts.^(29–31) Thus, we generated transgenic mice in which Wnt10b is expressed in mature osteoblasts as a means to better understand mechanisms by which Wnt signaling regulates postnatal bone mass.

MATERIALS AND METHODS

Mice

The Oc-Wnt10b transgene was constructed by excising the human osteocalcin promoter (3.5 kb) from pBS(K-) vector (gift from TL Clemens, University of Alabama at Birmingham) using *HindIII/XhoI* and inserting the promoter into the *HindIII/SalI* site of a pCRII (Invitrogen, Carlsbad, CA, USA) vector that was previously generated, by PCR, to contain mouse Wnt10b cDNA (1.2 kb; GenBank accession no. NM_011718) followed by the coding sequence for rabbit β -globin intron/poly A tail for transgene stability.⁽²⁶⁾ The *HindIII/XhoI* fragment of the Oc-Wnt10b transgene construct was purified and microinjected into fertilized C57BL/6 mouse eggs by the transgenic animal model core facility at the University of Michigan. Mice were screened for integration of the Oc-Wnt10b transgene by PCR using primers specific for the transgene, and nine

were positive. Based on radiographic and μ CT analyses, five showed some evidence of high bone mass; however, two founder males with increased bone mass by radiographic analysis were bred to wildtype C57BL/6 females to establish lines for subsequent analyses (Supplementary Fig. 1). Of these, line 492 showed very high bone mass. Only line 488, with a moderate increase in BMD, was extensively studied and is reported herein. The mouse colony for line 488 was maintained by crossing transgene-positive males with wildtype C57BL/6 females. Wnt10b^{-/-} mice were created by Timothy Lane (UCLA) and Philip Leder (Harvard University) and will be described elsewhere. Wnt10b^{-/-} mice were maintained on an FVB background. Wnt10b^{-/-} mice were generated by mating heterozygous males and females. For Oc-Wnt10b and Wnt10b^{-/-} mice, the respective control groups were obtained from same sex littermates. All animal studies were approved by the University Committee on Use and Care of Animals and were cared for by the Unit for Laboratory Animal Medicine at the University of Michigan.

Transgene expression

RNA was isolated from tissues with RNA Stat 60 (Tel-Test, Friendswood, TX, USA). Expression of Wnt10b transgene in tissues was measured by RNase protection assay, as described previously.^(26,32) The riboprobe hybridizes to both Wnt10b and the β -globin intron and contains the fragment between P1 and P2 as shown in the transgene schematic (Fig. 1).

Demineralization and histological analysis

At the indicated ages, mice were killed, and femurs, calvaria, and/or mandibles were isolated. The samples were fixed in 10% neutral buffered formalin overnight, decalcified in 0.5 mM EDTA (pH 7.33), embedded in paraffin, and sectioned at 5 μ m thickness. To assess tissue morphology, histological sections were stained with H&E. For measurement of cell proliferation, mice were injected with BrdU labeling reagent (100 μ l/10 g; Zymed Laboratories, San Francisco, CA, USA) 2 h before death, and histological sections were assessed using a BrdU staining kit (Zymed Laboratories). Histological sections were evaluated using image analysis software (Bioquant, Nashville, TN, USA). For each section evaluated, BrdU⁺ bone-lining cells and BrdU⁻ bone-lining cells were counted and percent of BrdU⁺ cells was calculated. To identify apoptotic cells, tissue sections were probed for DNA strand breaks using the In Situ Cell Death Detection Kit (Roche Pharmaceuticals, Nutley, NJ, USA). Briefly, dewaxed histological sections were incubated with TUNEL reaction solution for 1 h at 37°C in the dark. Sections were rinsed with PBS and counterstained with Hoechst nuclear dye. Sections were evaluated by fluorescence microscopy by counting TUNEL⁺ bone-lining cells versus Hoechst-positive bone-lining cells. To evaluate number of osteoclasts, tissue sections were stained for TRACP using a Leukocyte acid phosphatase staining kit (Sigma Aldrich Diagnostics, St Louis, MO, USA). TRACP⁺ osteoclasts were counted per millimeter bone surface using image analysis software (Bioquant).

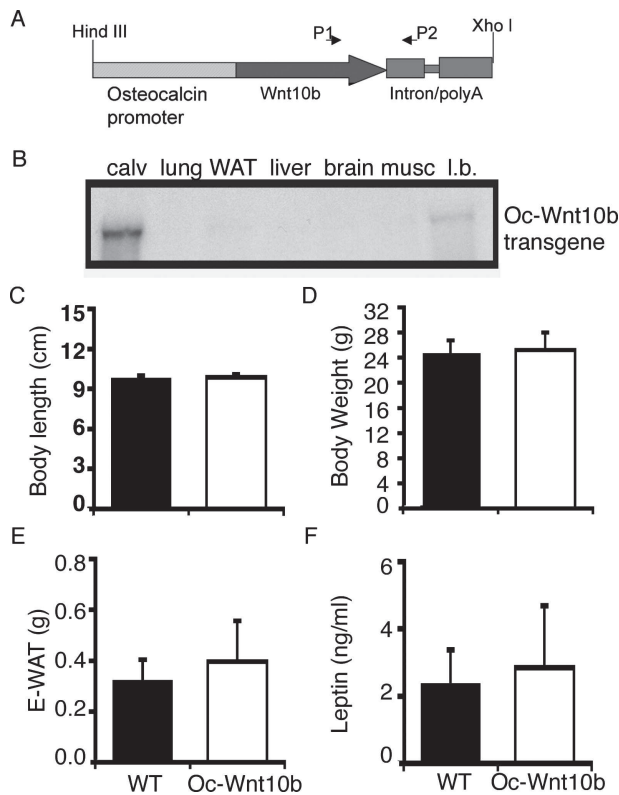


FIG. 1. General characteristics of Oc-Wnt10b mice. (A) Schematic of transgene in which the human osteocalcin promoter directs expression of mouse Wnt10b. The *HindIII/XhoI* fragment was injected into blastocysts and transgene-specific primers (P1 and P2) were used for identification of founders and subsequent genotyping of progeny by PCR. (B) Tissue-specific expression of Wnt10b transgene was evaluated by RNase protection assay in calvaria (Cal), lung, white adipose tissue (WAT), liver, brain, skeletal muscle (Mus), and femur (Fem) using a radiolabeled probe for the Wnt10b transgene spanning the P1–P2 fragment. (C) Body length from nose to anus, (D) total body weight, and (E) weight of epididymal white adipose tissue (E-WAT) was measured, and (F) serum leptin was assayed by ELISA in littermate control (WT) and Oc-Wnt10b male mice at 3 mo of age. Data are presented as mean \pm SD ($n = 8$). For C–F, differences were not observed between genotypes.

Double staining of mouse skeletons

General patterning of bone and cartilage was assessed by staining skeletons of newborn pups (P0) with alcian blue for cartilage and alizarin red for bone, as described in detail by Menengola et al.⁽³³⁾ After staining, bones were disarticulated and evaluated under a dissecting microscope for gross changes in cartilage and bone development.

Dynamic labeling of bone

Male mice at ~3 mo of age were given injections of 10 mg calcein green (Sigma Aldrich Diagnostics) per gram body weight 7 days apart and killed 2 days after the final injection. On the indicated days, two intraperitoneal injections were given 10 h apart with the first injection at 9:00 a.m. Femurs were dissected free of tissue, fixed in ethanol, and embedded in methyl methacrylate. Longitudinal sections of

5 μ m thickness were prepared for analysis. Measurements were performed on the entire marrow region within the cortical shell, between 0.1 and 1.5 mm proximal to the distal growth plate–metaphyseal junction, using an image analysis system (Osteomeasure, Atlanta, GA, USA). Trabecular area, perimeter, single- and double-labeling surfaces, inter-labeling width, osteoblast surface, and osteoclast number were measured, and trabecular number, thickness, separation, mineral apposition rate, and bone formation rate/tissue volume (BFR/TV) and surface (BFR/BS) referents were calculated as described previously.^(34,35)

μ CT and radiography

Femoral μ CT was as described previously,⁽³⁶⁾ using the stereology function of GE Medical Systems Microview software. 3D images were obtained for mandibles using μ CT. Radiographic images were obtained using a specimen radiography system (Faxitron, Wheeling, IL, USA), 25 kV for 15 s at $\times 2$ magnification.

Serology

For analysis of serum leptin, blood was collected at time of death, and serum was prepared for ELISA according to manufacturer's protocol (CrystalChem, Downers Grove, IL, USA). For analysis of serum C-terminal telopeptide of type I collagen (CTX), mice were fasted for 6 h, blood was collected from the saphenous vein, and serum was prepared for ELISA according to manufacturer's protocol (Nordic Bioscience Diagnostics). All serum samples were assayed in duplicate.

Statistical analysis

Unless indicated otherwise, data are presented as mean \pm SD. Data are considered significant at $p < 0.05$ by two-tailed Student's *t*-test analysis.

RESULTS

Generation of Oc-Wnt10b mice

To study the effects of canonical Wnt signaling on postnatal bone homeostasis, we generated transgenic mice that express Wnt10b in osteoblasts from the human osteocalcin promoter (Oc-Wnt10b; Fig. 1A). By PCR screening, nine mice integrated the transgene, and based on radiographic images, five showed some increase in bone mass. Although line 492 had considerably more trabecular bone than other Oc-Wnt10b lines (Supplementary Fig. 1), our interest was in characterizing a more physiological, rather than pathologic or superphysiological, state of bone remodeling. Thus, line 488, which has a more moderate increase in bone mass, was chosen for further characterization (Fig. 1). As expected, an RNase protection assay using a transgene specific probe revealed that the Oc-Wnt10b transgene (line 488) is expressed specifically in bone, including calvaria and femur of adult Oc-Wnt10b mice (Fig. 1B), without detectable expression in other tissues or in wildtype mice (data not shown). The transgene expression of Wnt10b in line 488 is ~5-fold higher than endogenous Wnt10b in calvaria and femoral marrow (data not shown). Body length (Fig. 1C) and weight (Fig. 1D) are not significantly different between

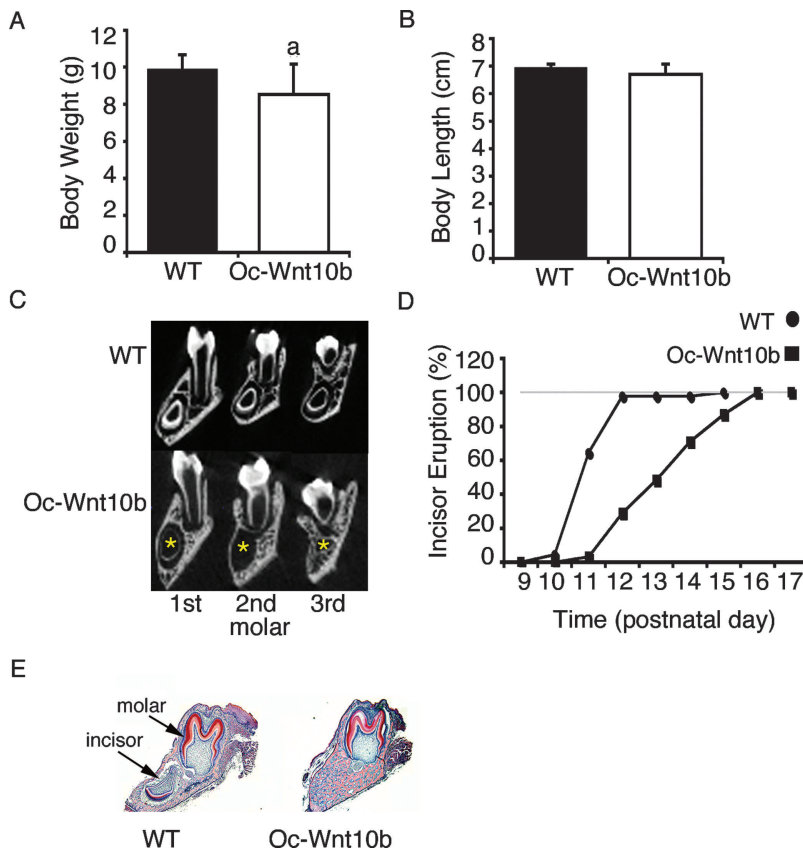


FIG. 2. Oc-Wnt10b mice have increased mandibular bone and delayed incisor development. (A) Body weight and (B) length of littermate control (WT) and Oc-Wnt10b mice at 3 wk of age. Data are presented as mean \pm SD ($n = 8$). ^a $p < 0.05$. (C) μ CT images of WT and Oc-Wnt10b mandibles, buccal-lingual, at the first, second, and third molars. *Difference in incisor development. (D) WT and Oc-Wnt10b mice were evaluated for eruption of mandibular incisors twice daily on days indicated. Eruption, as percent of total, is presented for WT (circles; $n = 43$) and Oc-Wnt10b (square; $n = 31$). (E) H&E-stained histological sections of WT and Oc-Wnt10b mandibles at 6 days of age.

wildtype and Oc-Wnt10b male mice at 3 mo of age. Importantly, the Oc-Wnt10b transgene does not alter weight of adipose tissues, including epididymal adipose tissue (Fig. 1E), and circulating levels of leptin are similar between genotypes (Fig. 1F). Thus, these transgenic mice provide a model to study mechanisms by which Wnt10b expressed exclusively by osteoblast lineage cells in bone directly increases bone mass.

Oc-Wnt10b mice have increased mandibular bone and delayed incisor development

Although differences were not observed in body size of Oc-Wnt10b mice at 3 mo of age (Figs. 1C and 1D) or in patterning of bone or cartilage at birth (Supplementary Figs. 2A and 2B), we observed that Oc-Wnt10b weanlings are slightly smaller in weight (Fig. 2A), but not in length (Fig. 2B), at 3 wk of age. Moreover, Oc-Wnt10b mice do not thrive on weaning unless water-softened or ground chow is provided, suggesting a defect or delay in tooth development. To assess molar and incisor development in Oc-Wnt10b mice at 3 wk of age, mandibles were isolated and scanned by μ CT. Although differences in first, second, and third molars between genotypes are not obvious (Fig. 2C), mineral density and thickness of incisors' enamel and dentin are compromised (Fig. 2C, note asterisks).

To confirm whether Oc-Wnt10b mice have delayed incisor eruption, mice were evaluated twice daily for eruption of incisors through soft tissue. In wildtype mice, 90% of incisors erupt by day 13 ($n = 43$), yet in Oc-Wnt10b mice,

<30% of incisors erupt by day 13, with ~20% erupting each additional day through day 16 ($n = 31$; Fig. 2D). Average day of incisor eruption was extended from 11.3 ± 0.8 days in controls to 13.6 ± 1.45 in Oc-Wnt10b mice ($p < 0.001$). To study whether delayed incisor development and eruption is caused by changes in early events within tooth formation, mandibles from postnatal day 6 were fixed and sectioned (Fig. 2E). Although histological analysis revealed that development of the first molar appears similar between genotypes, roots from mandibular incisors in Oc-Wnt10b mice have not extended to the first molar, presumably because of the high bone mass. By 6 wk of age, eruption of incisors in Oc-Wnt10b mice is largely complete, and incisor mineralization and extension through the mandible appear normal (data not shown).

Altered development of mandibular bone at 6 days of age in Oc-Wnt10b mice led us to evaluate development of calvaria, because both are derived from intramembranous osteogenesis. Interestingly, differences between histology of calvaria in littermate control and Oc-Wnt10b mice at 5 days or 1.5 mo of age were not observed (Supplemental Fig. 2C). In addition, histological analysis of suture lines provided no evidence for craniosynostosis.

Increased trabecular bone in femurs of Oc-Wnt10b mice

To assess whether Oc-Wnt10b mice also have changes in long bone architecture, femurs were isolated and scanned using μ CT. Visual inspection of μ CT images of male mice

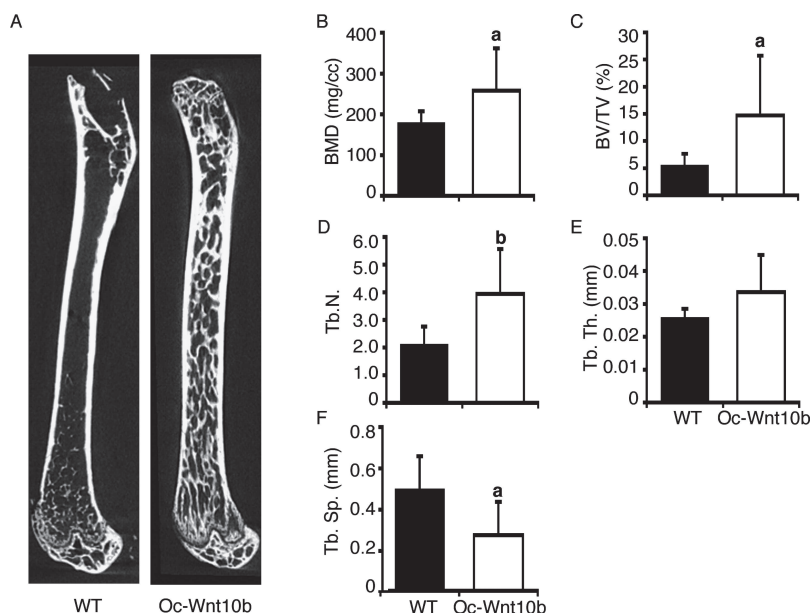


FIG. 3. Increased trabecular bone in Oc-Wnt10b mice. (A) μ CT images of femurs from littermate control (WT) and Oc-Wnt10b mice at 2.5 mo of age. (B–F) Morphometric properties of 1 mm³ of distal femur from wildtype (WT) and Oc-Wnt10b mice at 3 mo of age were analyzed for (B) BMD, (C) bone volume fraction (BV/TV, %), (D) trabecular number (Tr.N.), (E) trabecular thickness (Tb.Th.), and (F) trabecular spacing (Tb.Sp.). Data are presented as mean \pm SD. ^a $p < 0.05$; ^b $p < 0.001$ ($n = 6$).

at 3 mo of age reveals that Oc-Wnt10b mice have noticeably more trabecular bone throughout the entire endocortical compartment (Fig. 3A). Computed analyses of a 1-mm³ area within the distal metaphyses revealed a 1.4-fold increase in BMD (Fig. 3B) and a 2.5-fold elevation in bone volume fraction (BV/TV; Fig. 3C). The change in bone volume was caused by a 1.87-fold rise in trabecular number (Fig. 3D) without differences in trabecular thickness (Fig. 3E). As expected, an increase in both bone volume fraction and number of trabeculae was accompanied by reduced spacing between trabeculae (Fig. 3F). Last, cortical bone volume in control and Oc-Wnt10b mice, as assessed by μ CT and subsequent histomorphometric analyses, was similar (data not shown).

Dynamic changes in bone formation of Oc-Wnt10b and Wnt10b^{-/-} mice

To study how Wnt10b increases bone volume fraction, male mice at 3 mo of age were injected with calcein, 9 and 2 days before isolation and analysis of femurs. Calcein binds to calcium that is being incorporated into new bone and thus allows for assessment of dynamic changes that occur in bone formation by fluorescent microscopy. Static histomorphometric analyses of femoral sections indicate that Oc-Wnt10b mice have a 1.8-fold increase in bone volume fraction (BV/TV; Fig. 4A) and a 1.3-fold change increase in trabecular number (Tb.No; Fig. 4B), which corresponds with architectural findings by μ CT (Fig. 3). Dynamic histomorphometry reveals that expression of Wnt10b from the osteocalcin promoter significantly enhances rate of mineral apposition (MAR; Fig. 4D) and percent mineralizing surface (MS/BS; Fig. 4E). Together, increased rate and extent of mineralization in femurs of Oc-Wnt10b mice promote a 75% increase in bone formation rate (BFR/TV; Fig. 4F). Although increased rate of bone formation could be caused in part by enhanced activity of osteoblasts,⁽³⁷⁾ the ~1.4-fold increase in the percentage of bone surface occupied by os-

teoblasts (%Ob.Pm; Fig. 4C) and the increased mineralizing surface suggests that bone formation in Oc-Wnt10b mice is largely caused by elevated numbers of osteoblasts. Importantly, osteoclast variables, including number of osteoclasts/bone perimeter (WT, 1.21 ± 0.16 versus Tg, 1.12 ± 0.05 ; mean \pm SE) and percent osteoclasts on bone perimeter (WT, 1.78 ± 0.24 versus Tg, 1.62 ± 0.08), were not statistically different between genotypes.

Our prior analysis of Wnt10b^{-/-} mice indicated that endogenous Wnt10b is necessary for proper development and/or maintenance of trabecular bone mass.⁽²⁴⁾ To understand mechanisms whereby signaling by endogenous Wnt10b contributes to bone mass, we performed calcein-labeling experiments in 3-mo-old female Wnt10b^{-/-} mice in parallel to those described above for Oc-Wnt10b mice. As anticipated based on prior μ CT analyses,⁽²⁴⁾ histomorphometric measurements of femoral distal metaphyses from Wnt10b^{-/-} mice revealed a 30% decrease in bone volume fraction (Fig. 4A) and trabecular number (Fig. 4B). Although differences were not observed in osteoblast perimeter (Fig. 4C), MAR (Fig. 4D), or percent mineralizing surface (Fig. 4E), total bone formation rate was decreased in Wnt10b^{-/-} mice (Fig. 4F) because of a decrease in bone volume and trabecular number. Because differences in osteoblast number and mineralizing variables were not observed at this time-point, it leaves open the possibility that effects of Wnt10b are mediated earlier in development.

Mechanism by which Wnt10b signaling increases osteoblast number

The prominent bone phenotype in Oc-Wnt10b mice suggests that there is an essential underlying change in bone homeostasis that results in increased bone formation. Net bone formation could be caused by increased proliferation during osteoblastogenesis and/or increased lifespan or function of mature osteoblasts. Alternatively, increased bone formation could be the result of opposing effects in osteo-

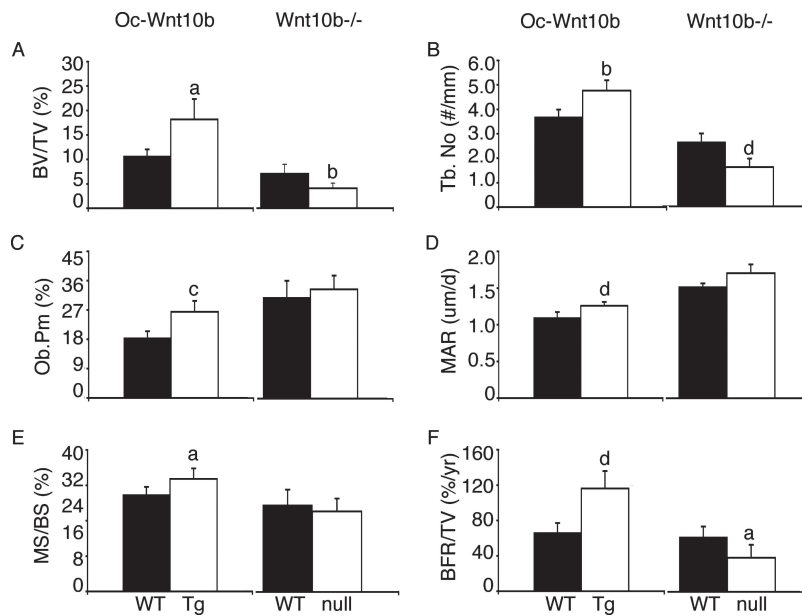


FIG. 4. Bone formation rates in Oc-Wnt10b and Wnt10b^{-/-} mice. Mineralization of bone was evaluated with calcein labeling in Oc-Wnt10b (Tg), Wnt10b^{-/-} (null), and littermate controls (WT) mice at 3 mo of age. Femurs were isolated and sectioned for static and dynamic histomorphometry. (A) Bone volume/total volume (BV/TV; %), (B) trabecular number (Tb.No.; #/mm), (C) osteoblast perimeter (Ob.Pm.; %), (D) mineral apposition rate (MAR; $\mu\text{m}/\text{d}$), (E) mineralizing surface/bone surface (MS/BS; %), and (F) bone formation rate/tissue volume (BFR/TV; %/yr) are presented as mean \pm SE. ^a $p < 0.05$, ^b $p < 0.01$, ^c $p < 0.005$, ^d $p < 0.001$ ($n = 6$).

clasts. To test whether Oc-Wnt10b mice have increased pre-osteoblast proliferation, mice at 3 and 6 wk of age were labeled with BrdU for 2 h before fixation. Mandibles, calvaria, and femurs were isolated and sectioned, and cellular replication was assessed. As expected, many cells within the marrow spaces of these bones have BrdU incorporation. However, overall numbers of BrdU-labeled osteoblasts, associated with bone surfaces, were low, and changes in percent BrdU⁺ cells in mandibles at 3 wk of age (Fig. 5A) and calvaria at 6 wk of age (Fig. 5B) were not statistically different than wildtype mice. Similarly, significant differences in BrdU labeling of osteoblasts were not found in femur at either age (data not shown). Wnt signaling is also known to protect against apoptosis⁽²⁹⁾; thus, to test whether expression of Wnt10b in osteoblasts decreases osteoblast turnover, sections of long bone were assayed for differences in apoptotic index by fluorescently labeling nicked DNA ends. Numbers of osteoblasts undergoing apoptosis were low, and differences were not detected between genotypes (data not shown).

An increase in bone mass could also be caused by a decrease in osteoclast number and/or activity. To determine whether Oc-Wnt10b mice have changes in numbers of osteoclasts, histological sections of Oc-Wnt10b and wildtype long bones from mice at 5 days, 3 wk, and 6 wk of age, were assayed for TRACP⁺ osteoclasts at 1.3 mm from the chondrocyte–osteoblast junction. Statistical analyses did not reveal significant changes in number of osteoclasts per millimeter of bone between WT and Oc-Wnt10b animals (Figs. 5C–5E). In some samples, there was a significant decrease in osteoclast number at 0.3 mm from the chondrocyte–osteoblast junction of femurs in Oc-Wnt10b mice at 5 days of age; however, this change was not consistent over time or on all bone surfaces. TRACP⁺ osteoclasts were also assessed in mandibles of control and Oc-Wnt10b mice at 3 and 6 wk of age. Although the number of osteoclasts decreases with age, differences were not observed between

genotypes (data not shown). Although Wnt10b did not alter osteoclast numbers, it is conceivable that osteoclast activity is impaired in Oc-Wnt10b mice. To assay for differences in osteoclast activity, serum was prepared from control and Oc-Wnt10b mice at 2 mo of age, and CTX levels were evaluated with ELISA (Fig. 5F). CTX is a collagen metabolite that is produced on type I collagen degradation, thus circulating levels of CTX correlate with total osteoclast number and bone-resorbing activity. Analyses of CTX levels in serum indicate that CTX is elevated in Oc-Wnt10b mice; however, this increase is proportional to the increase in osteoclast number associated with additional trabecular bone surface area in Oc-Wnt10b mice (Figs. 3 and 4). Thus, there is no evidence that increased bone formation is caused by reduced osteoclast number and/or activity. Instead, the main mechanisms whereby Wnt10b increases postnatal bone mass seem to be increased osteoblastogenesis, with a smaller effect on increased osteoblast mineralizing activity.

DISCUSSION

The Wnt pathway signals through autocrine and paracrine interactions to regulate many aspects of cell biology including development.⁽³⁸⁾ Wnt10b is 1 of 19 Wnts that activate the Wnt signaling pathway.⁽³⁹⁾ Thus far, only Wnt10b has been reported to play an endogenous role in postnatal maintenance of bone homeostasis.⁽²⁴⁾ However, because there is only a 20–30% reduction in trabecular bone in Wnt10b^{-/-} mice, there is likely at least one or even several other Wnts that help to maintain bone volume fraction. Indeed, redundancy and/or compensation within the Wnt signaling pathway, either by other Wnts or by factors that modulate Wnt signaling, may be an important control mechanism for maintaining homeostasis,⁽⁴⁰⁾ even with loss of one or more signaling components.

Our goal was to overexpress a physiologically relevant

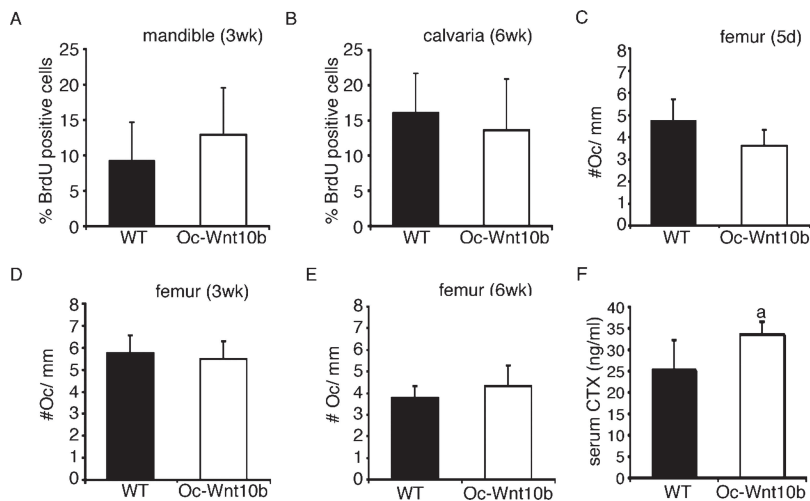


FIG. 5. Pre-osteoblast proliferation, osteoclast number, and osteoclast activity in Oc-Wnt10b mice. BrdU-positive and -negative bone-lining cells were counted in histological sections of mandible at 3 wk of age (A) and calvaria at 6 wk of age (B) from littermate control (WT) and Oc-Wnt10b mice with $n = 3$ with five sections counted/bone. TRACP⁺ osteoclasts per millimeter of bone surface were counted in histological sections of littermate control (WT) and Oc-Wnt10b femur at 5 days (C), 3 wk (D), and 6 wk (E) of age with $n = 3$ with five sections counted/bone. Serum CTX was assayed by ELISA in 2-month-old littermate control (WT; $n = 7$) and Oc-Wnt10b male mice ($n = 5$). Data are presented as mean \pm SD. ^a $p < 0.05$.

Wnt in mature mineralized tissue-associated cells including osteoblasts, cementoblasts, and odontoblasts⁽⁴¹⁾ and evaluate effects on development and postnatal bone remodeling. In our model system in which Wnt10b is expressed under control of the osteocalcin promoter, analyses of femoral bones indicated that Wnt10b stimulates an increase in osteoblast number and mineralizing activity (Fig. 4) without effects on preosteoblast proliferation, osteoblast turnover, and osteoclast activity (Fig. 5). Such findings provide evidence that targeting the Wnt signaling pathway might increase bone formation and bone volume fraction in the aged population or in postmenopausal women.

Although there is no difference in pre-osteoblast proliferation or osteoblast apoptosis at 3 and 6 wk of age (Fig. 5), there is an increase in overall osteoblast numbers per bone perimeter at 3 mo of age (Fig. 4). Thus, it seems that local expression of Wnt10b from osteoblasts induces differentiation of adjacent osteoblast precursor cells. We, and others, have shown previously that endogenous Wnt10b is expressed in mesenchymal precursor cells,^(24,42,43) and whereas enforced expression of Wnt10b ultimately results in induction of osteoblast transcription factors, including Runx2, Dlx5 and Osterix,⁽²⁴⁾ stimulation of osteoblastogenesis seems to be predominantly caused by rapid suppression of adipogenic transcription factors.⁽²⁵⁾ Moreover, expression of Wnt10b in mesenchymal precursor cells promotes mineralization in vitro and bone formation in vivo.⁽²⁴⁾ Although it remains possible that Wnt10b increases the pool of osteoblastic progenitors, it is highly likely that increased bone formation rate and osteoblast number is in part caused by effects of Wnt10b on osteoblastogenesis.

Our mouse model is one of several models that report changes in bone homeostasis caused by altered expression of components in the Wnt signaling pathway. Interestingly, bone phenotypes and mechanisms by which Wnt signaling increases bone formation are not consistent across models. For instance, mice deficient in the Wnt inhibitor sFRP1 have increased trabecular BMD only as adults.⁽⁴⁴⁾ This phenotype is caused by increases in osteoblast number and differentiation, as well as a decrease in osteoblast apoptosis. A mouse model that expresses a constitutively active

LRP5_(G171)⁽⁴⁵⁾ has high bone density by 5 wk of age because of an increased number of osteoblasts. Recently, two studies reported that constitutive expression of β -catenin in bone results in increased bone deposition; however, mice from both models die within 5 wk of birth.^(46,47) These mice have serious defects in osteoclast differentiation because of an increase in osteoprotegerin expression from osteoblasts. Moreover, knockout models for β -catenin in bone also suggest a defect in osteoclast differentiation as a primary cause for the bone phenotype.^(46,47) Thus, in vivo evidence suggests that regulation of Wnt signaling at the cell membrane (i.e., sFRP1, Wnt10b, and LRP5) induces an increase in bone mass through changes in osteoblast differentiation and activity, whereas regulation of Wnt signaling at the level of β -catenin increases bone mass through an osteoclast-mediated mechanism. Recent results show that Wnt signaling regulates mTOR activity and protein translation in a β -catenin-independent manner,⁽³⁷⁾ raising the possibility that Wnt signaling may also increase the mineralization capacity of osteoblasts through this mechanism. In addition, the severity of the bone phenotype in mice with altered expression of β -catenin may not be completely caused by effects on Wnt signaling, because β -catenin is also important for direct cell-to-cell interactions.⁽⁴⁸⁾ From these and other studies, regulation of Wnt signaling at the plasma membrane may be a viable target for increasing bone formation in osteopenic or osteoporotic patients.

Another salient phenotype of interest in Oc-Wnt10b mice is the delay in incisor development and eruption. This defect causes a noticeable change in overall growth of Oc-Wnt10b mice between 3 and 4 wk of age because of the compromised dental functions that prevent the animals from receiving sufficient nutrients from standard solid chow. This problem was completely circumvented, however, by providing a powdered diet. Although our knowledge of tooth development has increased dramatically during the past decades,⁽⁴⁹⁾ information on tooth type specification remains limited. Development of molars and incisors results from reciprocal signaling between dental epithelium and mesenchymal tissues, nevertheless, incisors possess several unique features. For instance, unlike mo-

lars, murine incisors continuously develop and erupt. Such a feature renders incisors susceptible to homeostasis of surrounding bone. Therefore, it is conceivable that the delay in incisor eruption seen in Oc-Wnt10b mice could be secondary to the increase in the adjacent craniofacial bone. The latter seems to be largely associated with increased osteoblast number and activity rather than repressed osteoclast functions. For example, TRACP staining of mandible at 3 wk of age (Fig. 5) shows that number of osteoclasts is not altered in Oc-Wnt10b mice. Alternatively, but not exclusively, Wnt10b may function through the genetic program intrinsic to incisor development to yield the observed results. Consistent with this idea, it has been reported that incisors possess distinct signaling molecules that only function during incisor development.⁽⁵⁰⁾ Indeed, more thorough analyses of Oc-Wnt10b mice are needed to determine the initiating events that lead to the increase in bone in the cranium and its effects on incisor development. Results from such analyses will not only provide valuable information on the role of Wnt10b signaling on tooth development in general but also on tooth type specification.

ACKNOWLEDGMENTS

This work was supported by grants from the National Institutes of Health to OAM (DK51563 and DK62876), KDH (RR00161 and AR49682), and HO (DE017439), as well as from the American Association of Endodontists to HO (N002846). Other support was from the Diabetes Research and Training Center (P60 DK20572) and the Nathan Shock Mutant and Transgenic Rodent Core. Fellowships to CNB were from Tissue Engineering and Regeneration Training Grant DE07057 and the American Physiological Society Porter Fellowship and to KMS from the Regenerative Sciences Training Grant DK070071. We thank David Fisher for μ CT scanning.

REFERENCES

1. Ralston SH, de Crombrughe B 2006 Genetic regulation of bone mass and susceptibility to osteoporosis. *Genes Dev* **20**:2492–2506.
2. Baron R, Rawadi G, Roman-Roman S 2006 Wnt signaling: A key regulator of bone mass. *Curr Top Dev Biol* **76**:103–127.
3. Gong Y, Slee RB, Fukai N, Rawadi G, Roman-Roman S, Reginato AM, Wang H, Cundy T, Glorieux FH, Lev D, Zacharin M, Oexle K, Marcelino J, Suwairi W, Heeger S, Sabatakos G, Apte S, Adkins WN, Allgrove J, Arslan-Kirchner M, Batch JA, Beighton P, Black GC, Boles RG, Boon LM, Borrone C, Brunner HG, Carle GF, Dallapiccola B, De Paepe A, Floege B, Halfhide ML, Hall B, Hennekam RC, Hirose T, Jans A, Juppner H, Kim CA, Keppler-Noreuil K, Kohlschuetter A, LaCombe D, Lambert M, Lemyre E, Letteboer T, Peltonen L, Ramesar RS, Romanengo M, Somer H, Steichen-Gersdorf E, Steinmann B, Sullivan B, Superti-Furga A, Swoboda W, van den Boogaard MJ, Van Hul W, Vikkula M, Votruba M, Zabel B, Garcia T, Baron R, Olsen BR, Warman ML 2001 LDL receptor-related protein 5 (LRP5) affects bone accrual and eye development. *Cell* **107**:513–523.
4. Hartikka H, Makitie O, Mannikko M, Doria AS, Daneman A, Cole WG, Ala-Kokko L, Sochett EB 2005 Heterozygous mutations in the LDL receptor-related protein 5 (LRP5) gene are associated with primary osteoporosis in children. *J Bone Miner Res* **20**:783–789.
5. Wehrli M, Dougan ST, Caldwell K, O'Keefe L, Schwartz S, Vaizel-Ohayon D, Schejter E, Tomlinson A, DiNardo S 2000 arrow encodes an LDL-receptor-related protein essential for Wingless signalling. *Nature* **407**:527–530.
6. Boyden LM, Mao J, Belsky J, Mitzner L, Farhi A, Mitnick MA, Wu D, Insogna K, Lifton RP 2002 High bone density due to a mutation in LDL-receptor-related protein 5. *N Engl J Med* **346**:1513–1521.
7. Kwee ML, Balemans W, Cleiren E, Gille JJ, Van Der Blij F, Sepers JM, Van Hul W 2005 An autosomal dominant high bone mass phenotype in association with craniosynostosis in an extended family is caused by an LRP5 missense mutation. *J Bone Miner Res* **20**:1254–1260.
8. Rickels MR, Zhang X, Mumm S, Whyte MP 2005 Oropharyngeal skeletal disease accompanying high bone mass and novel LRP5 mutation. *J Bone Miner Res* **20**:878–885.
9. Bhanot P, Brink M, Samos CH, Hsieh JC, Wang Y, Macke JP, Andrew D, Nathans J, Nusse R 1996 A new member of the frizzled family from *Drosophila* functions as a Wingless receptor. *Nature* **382**:225–230.
10. Mao B, Wu W, Li Y, Hoppe D, Stanek P, Glinka A, Niehrs C 2001 LDL-receptor-related protein 6 is a receptor for Dickkopf proteins. *Nature* **411**:321–325.
11. Pinson KI, Brennan J, Monkley S, Avery BJ, Skarnes WC 2000 An LDL-receptor-related protein mediates Wnt signalling in mice. *Nature* **407**:535–538.
12. Tamai K, Semenov M, Kato Y, Spokony R, Liu C, Katsuyama Y, Hess F, Saint-Jeannet JP, He X 2000 LDL-receptor-related proteins in Wnt signal transduction. *Nature* **407**:530–535.
13. Cong F, Schweizer L, Varmus H 2004 Wnt signals across the plasma membrane to activate the beta-catenin pathway by forming oligomers containing its receptors, Frizzled and LRP. *Development* **131**:5103–5115.
14. Mao J, Wang J, Liu B, Pan W, Farr GH III, Flynn C, Yuan H, Takada S, Kimelman D, Li L, Wu D 2001 Low-density lipoprotein receptor-related protein-5 binds to Axin and regulates the canonical Wnt signaling pathway. *Mol Cell* **7**:801–809.
15. Rubinfeld B, Albert I, Porfiri E, Fiol C, Munemitsu S, Polakis P 1996 Binding of GSK3 β to the APC-beta-catenin complex and regulation of complex assembly. *Science* **272**:1023–1026.
16. Aberle H, Bauer A, Stappert J, Kispert A, Kemler R 1997 beta-catenin is a target for the ubiquitin-proteasome pathway. *EMBO J* **16**:3797–3804.
17. Liu C, Li Y, Semenov M, Han C, Baeg GH, Tan Y, Zhang Z, Lin X, He X 2002 Control of beta-catenin phosphorylation/degradation by a dual-kinase mechanism. *Cell* **108**:837–847.
18. Molenaar M, van de Wetering M, Oosterwegel M, Peterson-Maduro J, Godsavage S, Korinek V, Roose J, Destree O, Clevers H 1996 XTcf-3 transcription factor mediates beta-catenin-induced axis formation in *Xenopus* embryos. *Cell* **86**:391–399.
19. Finch PW, He X, Kelley MJ, Uren A, Schaudies RP, Popescu NC, Rudikoff S, Aaronson SA, Varmus HE, Rubin JZ 1997 Purification and molecular cloning of a secreted, Frizzled-related antagonist of Wnt action. *Proc Natl Acad Sci USA* **94**:6770–6775.
20. Hsieh JC, Kodjabachian L, Rebbert ML, Rattner A, Smallwood PM, Samos CH, Nusse R, Dawid IB, Nathans J 1999 A new secreted protein that binds to Wnt proteins and inhibits their activities. *Nature* **398**:431–436.
21. Bafico A, Liu G, Yaniv A, Gazit A, Aaronson SA 2001 Novel mechanism of Wnt signalling inhibition mediated by Dickkopf-1 interaction with LRP6/Arrow. *Nat Cell Biol* **3**:683–686.
22. Takemaru K, Yamaguchi S, Lee YS, Zhang Y, Carthew RW, Moon RT 2003 Chibby, a nuclear beta-catenin-associated antagonist of the Wnt/Wingless pathway. *Nature* **422**:905–909.
23. Li X, Zhang Y, Kang H, Liu W, Liu P, Zhang J, Harris SE, Wu D 2005 Sclerostin binds to LRP5/6 and antagonizes canonical Wnt signaling. *J Biol Chem* **280**:19883–19887.
24. Bennett CN, Longo KA, Wright WS, Suva LJ, Lane TF, Hankenson KD, MacDougald OA 2005 Regulation of osteoblastogenesis and bone mass by Wnt10b. *Proc Natl Acad Sci USA* **102**:3324–3329.
25. Kang S, Bennett CN, Gerin I, Rapp LA, Hankenson KD, Mac-

- dougald OA 2007 Wnt signaling stimulates osteoblastogenesis of mesenchymal precursors by suppressing CCAAT/enhancer-binding protein [alpha] and peroxisome proliferator-activated receptor [gamma]. *J Biol Chem* **282**:14515–14524.
26. Longo KA, Wright WS, Kang S, Gerin I, Chiang SH, Lucas PC, Opp MR, MacDougald OA 2004 Wnt10b inhibits development of white and brown adipose tissues. *J Biol Chem* **279**:35503–35509.
 27. Ducy P, Amling M, Takeda S, Priemel M, Schilling AF, Beil FT, Shen J, Vinson C, Rueger JM, Karsenty G 2000 Leptin inhibits bone formation through a hypothalamic relay: A central control of bone mass. *Cell* **100**:197–207.
 28. Takeda S, Eleftheriou F, Levasseur R, Liu X, Zhao L, Parker KL, Armstrong D, Ducy P, Karsenty G 2002 Leptin regulates bone formation via the sympathetic nervous system. *Cell* **111**:305–317.
 29. Krishnan V, Bryant HU, MacDougald OA 2006 Regulation of bone mass by Wnt signaling. *J Clin Invest* **116**:1202–1209.
 30. Glass DA II, Karsenty G 2007 In vivo analysis of Wnt signaling in bone. *Endocrinology* **148**:2630–2634.
 31. Baron R, Rawadi G 2007 Wnt signaling and the regulation of bone mass. *Curr Osteopor Rep* **5**:73–80.
 32. MacDougald OA, Hwang CS, Fan H, Lane MD 1995 Regulated expression of the obese gene product (leptin) in white adipose tissue and 3T3-L1 adipocytes. *Proc Natl Acad Sci USA* **92**:9034–9037.
 33. Menegola E, Broccia ML, Giavini E 2001 Atlas of rat fetal skeleton double stained for bone and cartilage. *Teratology* **64**:125–133.
 34. Ma YF, Jee WS, Ke HZ, Lin BY, Liang XG, Li M, Yamamoto N 1995 Human parathyroid hormone-(1-38) restores cancellous bone to the immobilized, osteopenic proximal tibial metaphysis in rats. *J Bone Miner Res* **10**:496–505.
 35. Parfitt AM, Drezner MK, Glorieux FH, Kanis JA, Malluche H, Meunier PJ, Ott SM, Recker RR 1987 Bone histomorphometry: Standardization of nomenclature, symbols, and units. Report of the ASBMR Histomorphometry Nomenclature Committee. *J Bone Miner Res* **2**:595–610.
 36. Hankenson KD, Bain SD, Kyriakides TR, Smith EA, Goldstein SA, Bornstein P 2000 Increased marrow-derived osteoprogenitor cells and endosteal bone formation in mice lacking thrombospondin 2. *J Bone Miner Res* **15**:851–862.
 37. Inoki K, Ouyang H, Zhu T, Lindvall C, Wang Y, Zhang X, Yang Q, Bennett C, Harada Y, Stankunas K, Wang CY, He X, MacDougald OA, You M, Williams BO, Guan KL 2006 TSC2 integrates Wnt and energy signals via a coordinated phosphorylation by AMPK and GSK3 to regulate cell growth. *Cell* **126**:955–968.
 38. Logan CY, Nusse R 2004 The Wnt signaling pathway in development and disease. *Annu Rev Cell Dev Biol* **20**:781–810.
 39. Gordon MD, Nusse R 2006 Wnt signaling: Multiple pathways, multiple receptors, and multiple transcription factors. *J Biol Chem* **281**:22429–22433.
 40. Vertino AM, Taylor-Jones JM, Longo KA, Bearden ED, Lane TF, McGehee RE Jr, MacDougald OA, Peterson CA 2005 Wnt10b deficiency promotes coexpression of myogenic and adipogenic programs in myoblasts. *Mol Biol Cell* **16**:2039–2048.
 41. Franceschi RT 1999 The developmental control of osteoblast-specific gene expression: Role of specific transcription factors and the extracellular matrix environment. *Crit Rev Oral Biol Med* **10**:40–57.
 42. Ross SE, Hemati N, Longo KA, Bennett CN, Lucas PC, Erickson RL, MacDougald OA 2000 Inhibition of adipogenesis by Wnt signaling. *Science* **289**:950–953.
 43. Vaes BL, Decherer KJ, van Someren EP, Hendriks JM, van de Ven CJ, Feijen A, Mummery CL, Reinders MJ, Olijve W, van Zoelen EJ, Steegenga WT 2005 Microarray analysis reveals expression regulation of Wnt antagonists in differentiating osteoblasts. *Bone* **36**:803–811.
 44. Bodine PV, Zhao W, Kharode YP, Bex FJ, Lambert AJ, Goad MB, Gaur T, Stein GS, Lian JB, Komm BS 2004 The Wnt antagonist secreted frizzled-related protein-1 is a negative regulator of trabecular bone formation in adult mice. *Mol Endocrinol* **18**:1222–1237.
 45. Babji P, Zhao W, Small C, Kharode Y, Yaworsky PJ, Boussein ML, Reddy PS, Bodine PV, Robinson JA, Bhat B, Marzolf J, Moran RA, Bex F 2003 High bone mass in mice expressing a mutant LRP5 gene. *J Bone Miner Res* **18**:960–974.
 46. Glass DA II, Bialek P, Ahn JD, Starbuck M, Patel MS, Clevers H, Taketo MM, Long F, McMahon AP, Lang RA, Karsenty G 2005 Canonical Wnt signaling in differentiated osteoblasts controls osteoclast differentiation. *Dev Cell* **8**:751–764.
 47. Holmen SL, Zylstra CR, Mukherjee A, Sigler RE, Faugere MC, Boussein ML, Deng L, Clemens TL, Williams BO 2005 Essential role of beta-catenin in postnatal bone acquisition. *J Biol Chem* **280**:21162–21168.
 48. Mbalaviele G, Shin CS, Civitelli R 2006 Cell-cell adhesion and signaling through cadherins: Connecting bone cells in their microenvironment. *J Bone Miner Res* **21**:1821–1827.
 49. Thesleff I 2006 The genetic basis of tooth development and dental defects. *Am J Med Genet A* **140**:2530–2535.
 50. Mitsiadis TA, Angeli I, James C, Lendahl U, Sharpe PT 2003 Role of *Islet1* in the patterning of murine dentition. *Development* **130**:4451–4460.

Address reprint requests to:

Ormond A MacDougald, PhD

Department of Molecular and Integrative Physiology

7620 Medical Science II

1301 E. Catherine Street

Ann Arbor, MI 48106-0622, USA

E-mail: macdouga@umich.edu

Received in original form March 20, 2007; revised form August 13, 2007; accepted August 16, 2007.